INVARIANT AGGREGATOR FOR DEFENDING AGAINST FEDERATED BACKDOOR ATTACKS

Anonymous authors
Paper under double-blind review

ABSTRACT

Federated learning is gaining popularity as it enables training of high-utility models across several clients without directly sharing their private data. As a downside, the federated setting makes the model vulnerable to various adversarial attacks in the presence of malicious clients. Specifically, an adversary can perform backdoor attacks to control model predictions via poisoning the training dataset with a trigger. In this work, we propose a mitigation for backdoor attacks in a federated learning setup. Our solution forces the model optimization trajectory to focus on the invariant directions that are generally useful for utility and avoid selecting directions that favor few and possibly malicious clients. Concretely, we consider the sign consistency of the pseudo-gradient (the client update) as an estimation of the invariance. Following this, our approach performs dimension-wise filtering to remove pseudo-gradient elements with low sign consistency. Then, a robust mean estimator eliminates outliers among the remaining dimensions. Our theoretical analysis further shows the necessity of the defense combination and illustrates how our proposed solution defends the federated learning model. Empirical results on three datasets with different modalities and varying number of clients show that our approach mitigates backdoor attacks with a negligible cost on the model utility.

1 INTRODUCTION

Federated learning enables multiple distrusting clients to jointly train a machine learning model without sharing their private data directly. However, a rising concern in this setting is the ability of potentially malicious clients to perpetrate backdoor attacks. To this end, it has been argued that conducting backdoor attacks in a federated learning setup is practical (Shejwalkar et al., 2022) and can be effective (Wang et al., 2020). For instance, the adversary can connect to a federated learning system as a legitimate user and conduct a backdoor attack that forces the model to mispredict. The impact of such attacks is quite severe in many mission-critical federated learning applications. For example, anomaly detection is a common federated learning task where multiple parties (e.g., banks or email users) collaboratively train a model that detects frauds or phishing emails. Backdoor attacks allow the adversary to successfully circumvent these detection methods.

The most common backdoor attack embeds *triggers* in the data samples and forces the model to make an adversary-specified prediction when the trigger is observed (Liu et al., 2018; Bagdasaryan et al., 2020). Thus, an adversary can conduct a backdoor attack by generating a trigger that statistically correlates with a particular label. Once the adversary injects these trigger-embedded backdoor data samples into the training data, the model can entangle the trigger-label correlation and predict as the adversary specifies. Meanwhile, the backdoor attack often does not degrade the predictive accuracy on the benign samples, making backdoor detection difficult in practice (Wang et al., 2020).

In federated learning, the server aggregates only the client-level updates (a.k.a. pseudo-gradient or gradient for short) without control over the training procedure or any data samples. Such limited visibility of the federated learning server on the client-side training makes defending against backdoor attacks challenging. Common defenses against backdoor attacks aim at identifying the backdoor data samples or poisoned model parameters and usually require access to at least a subset of the training data (Tran et al., 2018; Li et al., 2021a), which is prohibitive for a federated learning server. Other defense methods against untargeted poisoning attacks that degrade the model utility

(Shejwalkar et al., 2022) are applicable but lack robustness against backdoor attacks, as discussed in Section 6.2.

Our approach. Our defense leverages the observation that learning from the poisonous data does not benefit the model on benign data and vice versa. Therefore, focusing on the invariant directions that are generally beneficial in the model optimization trajectory helps defending against the aforementioned backdoor attack (which often lead to non-invariant directions). To this end, we develop a defense by examining each *dimension* of the gradients on the server-side and checking whether the dimension-wise gradients point in the same *direction* across the clients. Here, a dimension-wise gradient can point to a positive or negative direction, or have a zero value. In the case of small learning rates and for a specific dimension, two gradients pointing in the same direction means that taking the direction of one gradient can benefit the other. As such, the *invariance* of a direction depends on how many dimension-wise gradients align with that direction. Following this intuition, we define the *sign consistency* of a dimension by the average gradient sign. The higher the sign consistency is, the more invariant direction the gradient dimension may have.

Designing such a method carefully selecting only the invariant gradient directions is non-trivial, especially given the non-i.i.d. gradient distributions across benign clients and the presence of malicious clients. Hence, our approach enforces two separate treatments for each gradient dimension. First, we employ an AND-mask (Parascandolo et al., 2021), a dimension-wise filter setting the gradient dimension with sign consistency below a given threshold to zero. However, this alone is not enough: the malicious clients can still use outliers to mislead the aggregation result in the remaining highly consistent dimensions. To address this issue, we propose using the trimmed-mean estimator (Xie et al., 2020b; Lugosi & Mendelson, 2021), as a means to remove the outliers. Our analysis suggests that the AND-mask complements the trimmed-mean estimator well, motivating their composition.

We support the proposed approach with a theoretical analysis under a conventional linear regime (Rosenfeld et al., 2021; Wang et al., 2022; Zhou et al., 2022; Manoj & Blum, 2021), showing that the composition of the AND-mask and the trimmed-mean estimator is necessary for defending against backdoor attacks. Our analysis starts with feature invariance and discusses the connection between feature invariance and gradient sign consistency. Then, we outline conditions under which trigger-based backdoor attacks can lead to non-invariant directions and decrease the sign consistency of a dimension. Further analysis results demonstrate the necessity for the combination of both the AND-mask and the trimmed-mean estimator. Simulation results in Appendix D.1 further verify our theoretical results.

Our empirical evaluation employs the strong edge-case backdoor attack (Wang et al., 2020), as detailed in Section 6.1, to test our defense. Empirical results on tabular (phishing emails), visual (CIFAR-10) (Krizhevsky, 2009; McMahan et al., 2017), and text (Twitter) (Caldas et al., 2018) datasets demonstrate that our method is effective in defending against backdoor attacks without degrading utility as compared to prior works. On average, our approach decreases the model accuracy on backdoor samples by 61.6% and only loses 1.2% accuracy on benign samples compared to the standard FedAvg aggregator (McMahan et al., 2017).

Contributions. Our contributions are as follows:

- We develop a combination of defenses using an AND-mask and the trimmed-mean estimator against the backdoor attack by focusing on the dimension-wise invariant directions in the model optimization trajectory.
- We theoretically analyze our strategy and demonstrate that a combination of an AND-mask and the trimmed-mean estimator is necessary in some conditions.
- We empirically evaluate our method on three datasets with varying modality, model architecture, and client numbers, as well as comparing the performance to existing defenses.

2 Related Work

Backdoor Attack. Common backdoor attacks aim at misleading the model predictions using a trigger (Liu et al., 2018). The trigger can be digital (Bagdasaryan et al., 2020), physical (Wenger et al., 2021), semantic (Wang et al., 2020), or invisible (Li et al., 2021b). Recent works extended

backdoor attacks to the federated learning setting and proposed effective improvements such as gradient scaling (Bagdasaryan et al., 2020) or generating edge-case backdoor samples (Wang et al., 2020). The state-of-the-art edge-case backdoor attack shows that using backdoor samples with low probability density on benign clients (i.e., unlikely samples w.r.t. the training distribution) are hard to defend in the federated learning setting.

Centralized Defense. There is a line of work proposing centralized defenses against backdoor attacks where the main aim is either detecting the backdoor samples (Tran et al., 2018) or purifying the model parameters that are poisoned (Li et al., 2021a). However, applying such centralized defense to federated learning systems is in practice infeasible due to limited access to the client data in many implementations.

Federated Defenses. Several recent works have attempted to defend against backdoor attacks in federated learning systems. Sun et al. (2019) shows that weak differential-private (weak-dp) federated averaging can mitigate the backdoor attack. However, the weak-dp defense is circumvented by the improved edge-case federated backdoor attack (Wang et al., 2020). Nguyen et al. (2021) suggest that the vector-wise cosine similarity can help detect malicious clients performing backdoor attacks. The vector-wise cosine similarity is insufficient when the backdoor attacks can succeed with few poisoned parameters, incurring little vector-wise difference (Wu & Wang, 2021). Other defenses against untargeted poisoning attacks (Blanchard et al., 2017; Xie et al., 2020b) lack robustness against the backdoor attack. Sign-SGD with majority vote (Bernstein et al., 2018; 2019) is similar to our approach, but it always takes the majority direction instead of focusing on the invariant directions. Section 6.2 discusses the limitation of previous defenses in more detail, along with the empirical evaluation. Unlike existing works, our defense encourages the model to pursue invariant directions in the optimization procedure.

Certification. Unlike the above discussed defenses, certification (Xie et al., 2021) aims at extinguishing backdoor samples within a neighborhood of a benign sample. A direct comparison between certification and our defense is not meaningful due to the different evaluation metrics. Certification considers the certification rate of benign samples as the metric, while our defense aims at reducing the accuracy of the backdoor samples. However, it would be interesting to investigate whether the proposed defense can ease the certification of a model.

3 Problem Setup

Notation. We assume a synchronous federated learning system, where N clients collaboratively train an ML model $f : \mathcal{X} \to \mathcal{Y}$ with parameter $\boldsymbol{w}$ coordinated by a server. An input to the model are the data samples $\boldsymbol{x} \in \mathcal{X} = \mathbb{R}^{\mathrm{d}}$ with d features indexed by k and a label y. There are $N' < \frac{N}{2}$ adversarial clients aiming at corrupting the ML model during training (Shejwalkar et al., 2022). The i^{th}, $i \in [1, ..., N]$, client has n_i data samples, being benign for $i \in [1, ..., N - N']$ or being adversarial for $i \in [N - N' + 1, ..., N]$. The synchronous federated learning is conducted in T rounds. In each round $t \in [1, ..., T]$, the server broadcasts a model parameterized by $\boldsymbol{w}_{t-1}$ to all the participating clients. We omit the subscript t while focusing on a single round. Then, the i^{th} client optimizes $\boldsymbol{w}_{t-1}$ on their local data samples indexed by j and report the locally optimized $\boldsymbol{w}_{t,i}$ to the server. We define pseudo-gradient $\boldsymbol{g}_{t,i} = \boldsymbol{w}_{t-1} - \boldsymbol{w}_{t,i}$ being the difference between the locally optimized model and the broadcasted model from the previous round. Note, for simplicity, that we often use the term "gradient" to refer to the pseudo-gradient. Once all gradients are uploaded, the server aggregates them and produces a new model with parameters $\boldsymbol{w}_t$ using the following rule: $\boldsymbol{w}_t = \boldsymbol{w}_{t-1} - \sum_{i=1}^{N} \frac{n_i}{\sum_{i=1}^{N} n_i} \boldsymbol{g}_{t,i}$. The goal of federated learning is to minimize a weighted risk function over the N clients: $F(\boldsymbol{w}) = \sum_{i=1}^{N} \frac{n_i}{\sum_{i=1}^{N} n_i} F_i(\boldsymbol{w}) = \sum_{i=1}^{N} \frac{n_i}{\sum_{i=1}^{N} n_i} \mathbb{E}_{\mathcal{D}_i}[\ell(f(x; \boldsymbol{w}), y)]$, where $\ell : \mathbb{R} \times \mathcal{Y} \to \mathbb{R}$ is a loss function. $\odot$ denotes the Hadamard product operator.

Threat Model. The adversary generates a backdoor data sample $\boldsymbol{x}'$ by embedding a trigger in a benign data sample $\boldsymbol{x}$ and correlating the trigger with a label y', which is different from the label y of the benign data sample. We use $\mathcal{D}'$ to denote the distribution of backdoor data samples. Then, the malicious clients connect to the federated learning system and insert backdoor data samples into the training set. Since the goal of federated learning is to minimize the risk over all clients' datasets, the model can entangle the backdoor while trying to minimize the risk over backdoor samples on the malicious clients. Appendix A visualizes some backdoor samples.

(a) Failure Mode 1 (AND-Mask)

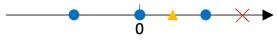

(b) Failure Mode 2 (Trimmed-mean)

Figure 1: Failure modes of AND-mask (a) and trimmed-mean estimator (b). Note that an aggregator fails if the malicious value flips the sign of the aggregation result compared to the true aggregate. Blue dots are benign values. Red crosses are malicious values. The orange box is an arithmetic mean and the orange triangle is a trimmed-mean. In (a), the adversary uses outliers to flip the sign of the arithmetic mean when the benign values have the same sign. (b) shows that the trimmed-mean estimator may bias toward the malicious value when the average is supposed to be zero, but the benign values have diverse signs.

To simplify tedious notation, we assume all users have the same number of samples i.e., $n_i = n_{i'}, \forall i \neq i'$.

4 METHOD

This section presents the proposed server-side defense operating on the gradients. We start with an overview of the idea, then introduce the two complementary components of our defense and outline the invariant aggregator steps.

4.1 OVERVIEW

In the proposed defense, we aim at finding invariant directions to optimize the federated learning model, such that the model is generally utilitarian for most of clients and can exclude the directions that benefit a subset of potentially malicious clients. Since our defense operates with the gradients, we consider the invariant direction from a first-order perspective (Parascandolo et al., 2021). Expanding the loss function around the current weight $\boldsymbol{w}$ on client i, for a parameter update $\boldsymbol{g}$, we have:

$$\mathbb{E}_{\mathcal{D}_i}[\ell(\boldsymbol{x}, y; \boldsymbol{w} + \boldsymbol{g})] = \mathbb{E}_{\mathcal{D}_i}[\ell(\boldsymbol{x}, y; \boldsymbol{w})] + \mathbb{E}_{\mathcal{D}_i}[\nabla_{\boldsymbol{w}} \ell(\boldsymbol{x}, y; \boldsymbol{w})]^\top \boldsymbol{g} + R_2(\boldsymbol{w} + \boldsymbol{g}), \tag{1}$$

where $R_2(\boldsymbol{w} + \boldsymbol{g})$ is a second-order Taylor remainder. With a reasonably small $\|\boldsymbol{g}\|$ (achievable with small learning rates), the remainder term $R_2(\boldsymbol{w} + \boldsymbol{g})$ is negligible and the change of the loss function mainly depends on the first-order gradient and the parameter update $\boldsymbol{g}$. Since learning the trigger benefits the malicious clients exclusively, there exists at least one gradient dimension k and one benign client $i \in \{1, ..., N - N'\}$ where $\mathbb{E}_{\mathcal{D}'}[\nabla_{\boldsymbol{w}_k} \ell(\boldsymbol{x}, y; \boldsymbol{w})] \neq 0$ and the dimension-wise gradient have inconsistent signs, i.e.,

$$\mathbb{E}_{\mathcal{D}_i}[\nabla_{\boldsymbol{w}_k} \ell(\boldsymbol{x}, y; \boldsymbol{w})] \times \mathbb{E}_{\mathcal{D}'}[\nabla_{\boldsymbol{w}_k} \ell(\boldsymbol{x}', y'; \boldsymbol{w})] \leq 0. \tag{2}$$

If the condition in Equation 2 is not true, then learning the trigger would always benefit the model on benign data, thereby contradicting common empirical observation. A more detailed analysis of the condition in Equation 2 is in Section 5.2. The proposed methods show how to treat the inconsistent signs and defend against the backdoor attack by only allowing invariant directions. A dimension-wise analysis is necessary because backdoor attacks can succeed by poisoning few inconsistent dimensions (Wu & Wang, 2021) without incurring much vector-wise difference, as Section 6.2 will show.

We consider two treatments for each gradient dimension to help the model avoid the direction specified by $\mathbb{E}_{\mathcal{D}'}[\nabla_{\boldsymbol{w}} \ell(\boldsymbol{x}', y'; \boldsymbol{w})]$: (Treatment 1) setting the dimension with inconsistent signs to zero using an AND-mask (Parascandolo et al., 2021) such that no client benefits or (Treatment 2) employing a robust mean estimator (e.g., trimmed-mean (Xie et al., 2020b)) to remove the malicious values that cause the inconsistent sign. To achieve a better result, we combine these two treatments to avoid their failure modes. The following examples illustrate the failure mode of each treatment and motivate the combination of defense.

Failure Mode 1. Figure 1a shows an example where the adversary may exploit a dimension by inserting outliers where the benign values have a consistent sign. The outliers can mislead the average toward the non-invariant direction. The robust mean estimator (treatment 2) can trim the outliers

and accurately estimate the mean. In contrast, treatment 1 can fail with a high sign consistency. Because it either lets the highly consistent dimension pass or has to be over-aggressive in zeroing out the dimensions, hurting the model's accuracy on benign data.

Failure Mode 2. Figure 1b shows some values with inconsistent signs, which treatment 1 can handle. However, this example can fail the robust mean estimator (treatment 2), whose result has the same sign as the malicious values.

The following sections shall detail the two treatments and discuss their complementary relationship.

4.2 AND-MASK

The AND-mask (Parascandolo et al., 2021) computes a dimension-wise mask by inspecting the sign consistency of each dimension across clients. For dimension k, the sign consistency is: $|\frac{1}{N}\sum_{i=1}^{N}\text{sign}(\boldsymbol{g}_{i,k})|$. If the sign consistency is below a given threshold τ, the mask element m_k is set to 0, otherwise, m_k is set to 1. The mask along dimension k is defined as:

Definition 1. (AND-Mask) For the k^{th} dimension in the gradient vector, the corresponding mask m_k is defined as:

$$m_k := \mathbf{1}\left[|\sum_{i=1}^{N}\text{sign}(\boldsymbol{g}_{i,k})| \geq \tau\right]. \tag{3}$$

Our defense then multiplies the mask m with the aggregated gradient $\bar{\boldsymbol{g}}$ element-wise, setting the inconsistent dimension to zero.

4.3 TRIMMED-MEAN

To complement the AND-mask, our defense broadcasts the trimmed-mean estimator to each gradient dimension. The trimmed-mean estimator alleviates the outlier issue by removing the subset of largest and smallest elements before computing the mean. The largest and smallest elements appear on the two tails of a sorted sequence. Next, we define order statistics and the trimmed mean estimator.

Definition 2. (Order Statistics) (Xie et al., 2020b) By sorting the scalar sequence $\{x_i : i \in \{1, ..., N\}, x_i \in \mathbb{R}\}$, we get $x_{1:N} \leq x_{2:N} \leq ... \leq x_{N:N}$, where $x_{i:N}$ is the i^{th} smallest element in $\{x_i : i \in \{1, ..., N\}\}$.

Then, the trimmed-mean estimator removes a $\alpha \times N$ elements from each tail of the sorted sequence.

Definition 3. (Trimmed Mean Estimator) (Xie et al., 2020b) For $\alpha \in [0, 1]$, the α-trimmed mean of the set of scalars $x_{i:N} \in \{1, ..., N\}$ is defined as follows:

$$\text{TrMean}(\{x_1, ..., x_N\}; \alpha) = \frac{1}{N - 2 \cdot \lceil \alpha \cdot N \rceil} \sum_{i=\lceil \alpha \cdot N \rceil + 1}^{N - \lceil \alpha \cdot N \rceil} x_{i:N}, \tag{4}$$

where $\lceil . \rceil$ denotes the ceiling function.

4.4 OUR APPROACH: INVARIANT AGGREGATOR

Algorithm 1 outlines the steps of our server-side defense that perform aggregation of invariant updates from the clients. The solution is composed of the AND-mask (treatment 1) and trimmed-mean estimator (treatment 2). Our defense applies the two components separately based on the sign consistency of each dimension with a threshold τ.

We show how these two components, i.e., the AND-mask and the trimmed-mean estimator, complement each other. Our analysis considers a single dimension and starts with the robustness of the trimmed mean estimator, which improves the robustness of the AND-mask against outliers. The following theorem extends the robustness guarantee of a modified trimmed-mean estimator (Lugosi & Mendelson, 2021), which is shown in Appendix B, to the conventional trimmed-mean estimator (Definition 3).

Algorithm 1 Server-side Defense

Input:
A set of reported gradients, $\{\boldsymbol{g}_i \mid i \in \{1, ..., N\}\}$;
Hyper-parameters τ, α;

Aggregator:

1: Compute the AND-mask $m := \mathbf{1}\left[|\sum_{i=1}^{N} \operatorname{sign}(\boldsymbol{g}_i)| \geq \tau\right]$ following Definition 1;
2: Compute the trimmed-mean $\bar{g} := \operatorname{TrMean}(\{\boldsymbol{g}_1, ..., \boldsymbol{g}_N\}; \alpha)$ under Definition 3;
3: **return** $m \odot \bar{g}$;

Theorem 4. *With the trimmed-mean estimator in Definition 3, for a given set of samples $x_1, ..., x_N$, with a corruption level $\eta = \frac{N'}{N}$ and a confidence level δ, set the trim level $\alpha = 8\eta + 12\frac{\log(\frac{4}{\delta})}{N}$, let $a = x_{\alpha N:N}$ and $b = x_{N-\alpha N:N}$ following Definition 2, x be a random variable with variance σ and $\bar{x}$ be the estimated mean, with probability at least $\sum_{i=N-\alpha N}^{N-N'} \binom{N-N'}{i} 0.99^i 0.01^{N-N'-i} c^{-4}(1 - 4e^{\frac{-\alpha N}{12}})$, we have:*

$$|\bar{x} - \mathbb{E}[x]| \leq (20\alpha + 10\sqrt{\alpha} + 2c)\sigma \tag{5}$$

The proof is in Appendix B. Theorem 4 bounds the estimation error of a trimmed-mean estimator, which can increase as the variable's variance increases. Multiple factors can increase the variance, such as non-i.i.d. federated data distribution and the stochastic gradient estimation process. In practice, a threat analysis is necessary to specify the maximum number of malicious clients to be tolerated, when the number of malicious clients is unknown. Our goal is to prevent the outliers from misleading the sign. Therefore, the estimation error to expectation ratio, $\frac{|\bar{x} - \mathbb{E}[x]|}{\mathbb{E}[x]}$, is particularly relevant. Since the estimator error for a given α depends on the variance, a high expectation-variance ratio, $\frac{\mathbb{E}[x]}{\sigma}$, is desirable. Then, we show that AND-mask identifies the elements with high expectation-variance ratios, avoiding the robustness degradation of the trimmed-mean estimator. The following theorem suggests that dimensions with a higher expectation-variance ratio have high probabilities of passing AND-mask, and increasing the mask threshold τ increases the chance of filtering out dimensions with low expectation-variance ratios.

Theorem 5. *Given a non-zero expectation-variance ratio $\phi = \frac{\mathbb{E}[x]}{\sigma}$, N' malicious elements, with probability at most $\sum_{i=N-2N'-\tau N}^{\min(N, N-2N'+\tau N)} \binom{N-N'}{i} \phi^{-2i}$, the sign consistency is below τ.*

Appendix B provides the proof. For the $\phi = 0$ case, we may use the probability of the estimated gradient sign being the same as the malicious gradient to replace ϕ^{-2}. We do not propose directly using the sample mean-variance ratio due to a potential issue: using the sample mean-variance ratio can be over-aggressive when the benign value has a consistent sign but varying magnitudes. Our ablation study in Appendix D.2 shows that AND-mask can preserve more utility than the sample mean-variance ratio when combined with the trimmed-mean estimator.

5 Robustness analysis for a simplified model

To further motivate our approach, we consider a more direct robustness analysis for a specific generative model. This analysis discusses how the features impact the gradient sign consistency, when the two failure modes in Section 4.1 appear, and why we need a combination of defenses guaranteed by Theorems 4 and 5. First, we outline some preliminaries useful for this analysis.

5.1 Preliminaries

We consider a binary prediction task $y \in \{0, 1\}$ with a linear model $h(\boldsymbol{x}) = \boldsymbol{w}^\top \boldsymbol{x}$ and a decision rule $\hat{y} = \mathbf{1}_{\boldsymbol{w}^\top \boldsymbol{x} \geq 0}(\boldsymbol{w}^\top \boldsymbol{x})$. The training procedure uses a Sigmoid activation function $s(z) = \frac{1}{1+e^{-z}}$ and a logistic loss function $\ell(z, y) = -y \cdot \log(z) - (1 - y) \cdot \log(1 - z)$, where $z = h(\boldsymbol{x})$.

Data Model. We assume that the samples per class are balanced on benign clients. The data samples come from a non-i.i.d. Gaussian distribution with a diagonal covariance matrix. On the i^{th} client, for the k^{th} feature, we have:

$$\boldsymbol{x}_k \sim \mathcal{N}\Big((2y - 1) \cdot \boldsymbol{\mu}_{i,k}, \boldsymbol{\sigma}_{i,k}\Big). \tag{6}$$

Backdoor Attack. We consider a single feature backdoor attack where the trigger is the k^{th} feature $\boldsymbol{x}_k$. A backdoor using a specific feature is common (Wang et al., 2020). To backdoor images, the adversary often selects a pixel pattern or semantic pattern (e.g., blue color on airplanes). For text data, the trigger could be a dedicated set of characters . The malicious clients attack in collusion using the same backdoor samples, meaning that $\boldsymbol{\mu}_{i,k} = \boldsymbol{\mu}_{i',k} \neq 0, \forall i, i' \in \{N - N' + 1, N\}$. To simplify the notation, we omit the subscript i for simplicity while focusing on a single client. Since the trigger is not useful or does not appear on benign clients, we assume $\boldsymbol{\mu}_{i,k} = 0, \forall i \in \{1, N - N'\}$

Objective. The backdoor attack is effective if the model entangles the trigger-label correlation. For a non-zero $\boldsymbol{\mu}_k$ of the trigger $\boldsymbol{x}_k$, $\boldsymbol{w}_k \boldsymbol{\mu}_k > 0$ is a necessary condition for a model to entangle the trigger-label correlation. Therefore, in the case when $\boldsymbol{\mu}_k > 0$, avoiding $\boldsymbol{w}_k$ from increasing and enforcing $\boldsymbol{w}_k$ to decrease while $\boldsymbol{w}_k > 0$ can mitigate the backdoor attack.

5.2 Connecting Features to Gradients

We define the invariance of a feature by measuring its feature-label correlation (e.g., positive or negative) consistency across clients.

Definition 6. For a given feature k, its invariance p is defined as: $p = \left| \frac{1}{N} \cdot \sum_{i=1}^{N} \text{sign}(\boldsymbol{\mu}_{i,k}) \right|$.

Similarly, we define the sign consistency of a gradient dimension k:

Definition 7. With a linear model $h(x) = \boldsymbol{w}^\top \boldsymbol{x}$, a Sigmoid activation function s, and N clients, a q-consistent gradient w.r.t. $\boldsymbol{w}_k$ satisfies: $\left| \frac{1}{N} \cdot \sum_{i=1}^{N} \text{sign}\Big(\mathbb{E}_{\boldsymbol{x}, y \sim \mathcal{D}_i} \left[\nabla_{\boldsymbol{w}_k} \ell(s(\boldsymbol{w}^\top \boldsymbol{x}), y) \right] \Big) \right| = q$.

Under Definitions 6 and 7, we discuss the connection between feature invariance and dimension-wise gradient sign consistency. First, we need to analyze the behavior of the gradient sign per client.

Theorem 8. *For a linear model with a Sigmoid activation function s and the logistic loss ℓ, under our Gaussian data model, on the k^{th} feature with a non-zero $\boldsymbol{\mu}_k$, if $\boldsymbol{w}_k \boldsymbol{\mu}_k \leq 0$, we have* $\text{sign}\Big(\mathbb{E}_{\boldsymbol{x}, y \sim \mathcal{D}_i} \left[\nabla_{\boldsymbol{w}_k} \ell(s(\boldsymbol{w}^\top \cdot \boldsymbol{x}), y) \right] \Big) = \text{sign}(\boldsymbol{\mu}_k)$. *In addition, if $\boldsymbol{\mu}_k = 0$, we have* $\text{sign}\Big(\mathbb{E}_{\boldsymbol{x}, y \sim \mathcal{D}_i} \left[\nabla_{\boldsymbol{w}_k} \ell(s(\boldsymbol{w}^\top \cdot \boldsymbol{x}), y) \right] \Big) = \text{sign}(\boldsymbol{w}_k)$.

The proof is provided in Appendix B. The result in Theorem 8 is intuitive. With a non-zero $\boldsymbol{\mu}_k$, if $\text{sign}(\boldsymbol{w}_k)$ agrees with $\text{sign}(\boldsymbol{\mu}_k)$, the gradient sign can be indefinite because the weight $\boldsymbol{w}_k$ can be either larger or smaller than the optimal $\boldsymbol{w}_k^*$. Otherwise, the gradient has the same sign as $\boldsymbol{\mu}_k$. If $\boldsymbol{\mu}_k = 0$, $\boldsymbol{w}_k$ shall shrink to 0. Then, we outline the conditions that lead to inconsistent signs.

Corollary 9. *Under Theorem 8, suppose $\boldsymbol{x}_k$ represents the trigger, $\boldsymbol{\mu}_k = 0$ on the $N - N'$ benign clients and the N' malicious clients share the same non-zero $\boldsymbol{\mu}_k$, if $\boldsymbol{w}_k = 0$, the gradient w.r.t. $\boldsymbol{w}_k$ is $\frac{N'}{N}$-consistent. In addition, if $\boldsymbol{w}_k \boldsymbol{\mu}_k > 0$, the gradient w.r.t. $\boldsymbol{w}_k$ is at least $(1 - \frac{N'}{N})$-consistent. The gradient w.r.t. $\boldsymbol{w}_k$ is 1-consistent if $\boldsymbol{w}_k \boldsymbol{\mu}_k < 0$.*

Counting the gradient signs yields the result. Corollary 9 suggests that if $\boldsymbol{w}_k \boldsymbol{\mu}_k > 0$ and the model entangles the backdoor, the expected gradient w.r.t. $\boldsymbol{w}_k$ can align with $\boldsymbol{\mu}_k$ on malicious clients and conflict with $\boldsymbol{\mu}_k$ on benign clients. Then, employing the trimmed-mean estimator to remove the malicious values can recover the invariant direction pointed by benign clients (Theorem 4) and thereby shrink $\boldsymbol{\mu}_k$. If $\boldsymbol{\mu}_k = 0$, using AND-mask can mask out the gradients w.r.t. $\boldsymbol{w}_k$ from the malicious clients (Theorem 5). If $\boldsymbol{w}_k$ remains 0, the model parameterized by $\boldsymbol{w}$ is robust to the trigger on $\boldsymbol{x}_k$. It is worth noting that the gradients w.r.t. $\boldsymbol{w}_k$ is 1-consistent and align to $\boldsymbol{\mu}_k$ when $\boldsymbol{w}_k \boldsymbol{\mu}_k < 0$. Such a consistent gradient may overshoot and flip the sign of $\boldsymbol{w}_k$. Reducing the learning rate can alleviate overshooting and the trimmed-mean estimator will guarantee $\boldsymbol{w}_k$ to shrink after the overshooting.

Connection to Failure Modes. If $\boldsymbol{w}_k \boldsymbol{\mu}_k > 0$, the gradients w.r.t. $\boldsymbol{w}_k$ have a consistent but non-zero expectation among benign clients, causing the failure mode 1 in Section 4.1. On the other hand, the gradient variance can diversify the estimated gradient sign and cause the failure mode 2.

Appendix D.1 further provides simulation results under the linear regime (Section 5.1), showing that the AND-mask can prevent the adversary from exploiting $\boldsymbol{w}_k$ and the trimmed-mean estimator helps shrink $\boldsymbol{w}_k$.

6 EXPERIMENTS

We evaluate our defense on three realistic tasks on three different data types: (1) object recognition with visual data, (2) sentiment analysis with text data, and (3) phishing email detection with tabular data. We employ the state-of-the-art edge-case backdoor attack (Wang et al., 2020) to generate backdoor samples and evaluate of defense and existing defenses against it.

Additional Results. The simulations, an ablation study, an evaluation of the hyper-parameter sensitivity, evaluations with additional attack strategies, and empirical verifications of the two failure modes can be found in the Appendix D.

6.1 EXPERIMENTAL SETUP

We briefly summarize our setup and report more details in Appendix C.

Metrics. Our experiments employ two metrics: the main task accuracy (Acc_M) estimated on the benign samples and the backdoor task accuracy (Acc_B) over backdoor samples. A defense is designed to reduce the model's accuracy on backdoor task and maintain the utility on the main task.

Datasets. The visual data of the object detection task and text data of the sentiment analysis task are from CIFAR-10 (Krizhevsky, 2009; McMahan et al., 2017) and Twitter (Caldas et al., 2018), respectively. Each phishing email data sample has 45 standardized numerical features of the sender that represent the sender reputation scores. A large reputation score may indicate a phishing email. The reputation scores come from peer-reviewers in a reputation system (Jøsang et al., 2007). The adversary may use malicious clients to manipulate the reputation.

Federated Learning Setup. We consider horizontal federated learning (Kairouz et al., 2021) where the clients share the same feature and label spaces. The number of clients are 100 for the three tasks. The server sample 20 clients at each round on the CIFAR-10 and phishing email experiments. We reduce the sampled client number to 15 on the Twitter experiment due to limited hardware memory.

Backdoor Attack Setup. The adversary employs the edge-case backdoor attack, where it selects the data samples with low marginal probability in their data distribution to create backdoor samples. The visual and text backdoor samples follow the previous work (Wang et al., 2020). For the tabular data, we select the 38^{th} feature (reputation), whose value is 0 on most of the data samples. Then, we let the adversary manipulate the 38^{th} feature to 0.2 that has a low probability density on phishing emails and flip the label to non-phishing.

The adversary can control 20% clients on the CIFAR-10 and phishing email experiments and 10% clients on the Twitter experiment. Section 6.2 explains the different experiment configurations. Such an adversary is considered strong in practice (Shejwalkar et al., 2022). We consider a strong adversary because defending against strong adversary yields robustness against weak adversary, whose effectiveness is already shown (Wang et al., 2020). The adversary only uses backdoor samples during training.

6.2 RESULT AND COMPARISON TO PRIOR WORKS

Our results. Table 1 summarizes the performance of each defense on three tasks. Our approach decreases the backdoor task accuracy by 61.6% on average. The edge-case backdoor attack on the text sentiment analysis task (Twitter) is more difficult to defend and our approach mitigates the accuracy increase on the backdoor task by 41.7%. We hypothesize that the text sentiment analysis task has few invariant and benign features. For example, the shape features (Sun et al., 2021) in object classification tasks can be invariant across objects. In contrast, the sentiment largely depends on the entire sentence instead of a few symbols or features. Then, we discuss the limitations of prior defenses.

Vector-wise. Common vector-wise defenses such as Krum estimate pair-wise similarities in terms of Euclidean distance (Blanchard et al., 2017) (Krum and multi-Krum) of cosime similarity (Nguyen et al., 2021) (multi-Krum_C) between each gradient and others. The gradients that are dissimilar to others are removed. The vector-wise view is insufficient for defending against backdoor attacks because backdoor attacks can succeed by manipulating a tiny subset of parameters (e.g. 5%) (Wu & Wang, 2021) without incurring much vector-wise difference. In practice, we observe that the malicious gradients can get high similarity scores and circumvent vector-wise defenses.

Table 1: Accuracy of Aggregators under Edge-case Backdoor Attack. Our approach reduces the model accuracy on backdoor samples by 61.7% on average, mitigating the backdoor attack, and achieves a comparable utility on benign samples as the standard FedAvg aggregator.

Method	CIFAR-10		Twitter		Phishing	
	Acc_M	Acc_B	Acc_M	Acc_B	Acc_M	Acc_B
FedAvg	.679 ± .001	.717 ± .001	.722 ± .001	.440 ± .001	.999 ± .001	.999 ± .001
Krum	.140 ± .001	.275 ± .012	.579 ± .001	.766 ± .002	.999 ± .001	.999 ± .001
Multi-Krum	.541± .002	.923 ± .021	.727 ± .001	.656 ± .008	.999 ± .001	.999 ± .001
Multi-Krum$_C$	.681 ± .002	.821 ± .001	.594 ± .002	.701 ± .001	.999 ± .001	.333 ± .333
Trimmed-Mean	.687 ± .001	.512 ± .002	.728 ± .001	.640 ± .016	.999 ± .001	.999 ± .001
Krum Trimmed-Mean	.682 ± .001	.607 ± .002	.727 ± .001	.641 ± .001	.999 ± .001	.999 ± .001
Sign-SGD	.301 ± .005	**.000 ± .001**	.610 ± .003	.751 ± .076	.999 ± .000	.667 ± .333
Weak-DP	.454 ± .003	.828 ± .003	.667 ± .001	.374 ± .002	.999 ± .001	.999 ± .001
Freezing Layers	.415 ± .001	.572 ± .002	N\A	N\A	N\A	N\A
FoolsGold	.667 ± .001	.109 ± .001	.726 ± .002	.357 ± .001	.999 ± .001	.999 ± .001
RFA	.685 ± .001	.853 ± .002	.718 ± .001	.704 ± .002	.999 ± .001	.999 ± .001
SparseFed	.662 ± .001	.984 ± .001	.667 ± .001	.608 ± .002	.999 ± .001	.999 ± .001
No Attack	.718 ± .001	.000 ± .001	.731 ± .001	.095 ± .001	.999 ± .001	.000 ± .001
Ours	.677 ± .001	**.001 ± .001**	.687 ± .001	**.296 ± .003**	.999 ± .001	**.000 ± .001**

Note: The numbers are average accuracy over three runs. Variance is rounded up.

Dimension-wise. Failure mode 2 in Section 4.1 shows the limitation of the trimmed-mean estimator, which was the most effective defense against the edge-case backdoor attack. We also include Sign-SGD with majority vote (Bernstein et al., 2019) as a defense, which binarizes the gradient and takes the majority vote as the aggregation result. However, Sign-SGD struggles to train a large federated model (e.g., Resnet-18 on CIFAR-10) and can suffer from failure mode 1 where the clients have diverse signs. Then, the adversary can put more weight on one side and mislead the voting result.

Combination. A naive combination of multi-Krum and the trimmed-mean estimator fails to defend against the backdoor attack because neither multi-Krum nor the trimmed-mean estimator avoids the failure mode of the other.

Weak-DP. The weak-DP defense (Sun et al., 2019) first bounds the gradient norms, then add additive noise (e.g., Gaussian noise) to the gradient vector. The edge-case backdoor attack can work without scaling up the gradients, circumventing the norm bounding. For the additive noise, we hypothesize that in some dimensions, the difference between malicious and benign gradients can be too large for the Gaussian noise to blur their boundary.

Freezing Layers. Since we employ a pre-trained Resnet-18 (He et al., 2016) on CIFAR-10, freezing the convolution layers may avoid entangling the trigger. However, this approach lacks empirical robustness, possibly because the adversary can use semantic features (e.g., blue color on airplanes) that the pre-trained model already learns as triggers.

Advanced Defenses. FoolsGold (Fung et al., 2020) down-weights an update if that update has a high cosine similarity with another update. There are many ways to diversify updates. Malicious clients may leverage the stochastic gradient estimation process or mix backdoor samples with benign samples, whose distribution can differ across clients. RFA (Pillutla et al., 2022) computes geometric medians as the aggregation result, which is shown to be ineffective (Wang et al., 2020). SparseFed (Panda et al., 2022) only accepts elements with large magnitude in the aggregation results. However, benign and malicious updates can contribute to large magnitudes.

7 Conclusion and Future Work

This paper shows how to defend against backdoor attacks by focusing on the invariant directions in the model optimization trajectory. Enforcing the model to follow the invariant direction requires AND-mask to compute the sign-consistency of each gradient dimension, which estimates how invariant a dimension-wise direction can be, and use the trimmed-mean estimator to guarantee the model follows the invariant direction within each dimension. Both theoretical and empirical results demonstrate the combination of AND-mask and the trimmed-mean estimator is necessary and effective. Further defending against more advanced backdoor attacks such as invisible backdoors that add calibrated noise to all the features (Li et al., 2021b; Manoj & Blum, 2021) can be interesting.

REFERENCES

Eugene Bagdasaryan, Andreas Veit, Yiqing Hua, Deborah Estrin, and Vitaly Shmatikov. How to backdoor federated learning. In Silvia Chiappa and Roberto Calandra (eds.), *Proceedings of the Twenty Third International Conference on Artificial Intelligence and Statistics*, volume 108 of *Proceedings of Machine Learning Research*, pp. 2938–2948. PMLR, 26–28 Aug 2020. URL https://proceedings.mlr.press/v108/bagdasaryan20a.html.

Jeremy Bernstein, Yu-Xiang Wang, Kamyar Azizzadenesheli, and Animashree Anandkumar. signSGD: Compressed optimisation for non-convex problems. In Jennifer Dy and Andreas Krause (eds.), *Proceedings of the 35th International Conference on Machine Learning*, volume 80 of *Proceedings of Machine Learning Research*, pp. 560–569. PMLR, 10–15 Jul 2018. URL https://proceedings.mlr.press/v80/bernstein18a.html.

Jeremy Bernstein, Jiawei Zhao, Kamyar Azizzadenesheli, and Anima Anandkumar. signsgd with majority vote is communication efficient and fault tolerant. In *ICLR*, 2019.

Peva Blanchard, El Mahdi El Mhamdi, Rachid Guerraoui, and Julien Stainer. Machine learning with adversaries: Byzantine tolerant gradient descent. In *NIPS*, 2017.

Sebastian Caldas, Peter Wu, Tian Li, Jakub Konecný, H. B. McMahan, Virginia Smith, and Ameet S. Talwalkar. Leaf: A benchmark for federated settings. *ArXiv*, abs/1812.01097, 2018.

Clement Fung, Chris J. M. Yoon, and Ivan Beschastnikh. The limitations of federated learning in sybil settings. In *23rd International Symposium on Research in Attacks, Intrusions and Defenses (RAID 2020)*, pp. 301–316, San Sebastian, October 2020. USENIX Association. ISBN 978-1-939133-18-2. URL https://www.usenix.org/conference/raid2020/presentation/fung.

Kaiming He, X. Zhang, Shaoqing Ren, and Jian Sun. Deep residual learning for image recognition. *2016 IEEE Conference on Computer Vision and Pattern Recognition (CVPR)*, pp. 770–778, 2016.

Audun Jøsang, Roslan Ismail, and Colin Boyd. A survey of trust and reputation systems for online service provision. *Decis. Support Syst.*, 43:618–644, 2007.

Peter Kairouz, H. B. McMahan, Brendan Avent, Aurélien Bellet, Mehdi Bennis, Arjun Nitin Bhagoji, Keith Bonawitz, Zachary B. Charles, Graham Cormode, Rachel Cummings, Rafael G. L. D'Oliveira, Salim Y. El Rouayheb, David Evans, Josh Gardner, Zachary Garrett, Adrià Gascón, Badih Ghazi, Phillip B. Gibbons, Marco Gruteser, Zaïd Harchaoui, Chaoyang He, Lie He, Zhouyuan Huo, Ben Hutchinson, Justin Hsu, Martin Jaggi, Tara Javidi, Gauri Joshi, Mikhail Khodak, Jakub Konecný, Aleksandra Korolova, Farinaz Koushanfar, Oluwasanmi Koyejo, Tancrède Lepoint, Yang Liu, Prateek Mittal, Mehryar Mohri, Richard Nock, Ayfer Özgür, R. Pagh, Mariana Raykova, Hang Qi, Daniel Ramage, Ramesh Raskar, Dawn Xiaodong Song, Weikang Song, Sebastian U. Stich, Ziteng Sun, Ananda Theertha Suresh, Florian Tramèr, Praneeth Vepakomma, Jianyu Wang, Li Xiong, Zheng Xu, Qiang Yang, Felix X. Yu, Han Yu, and Sen Zhao. Advances and open problems in federated learning. *ArXiv*, abs/1912.04977, 2021.

Alex Krizhevsky. Learning multiple layers of features from tiny images. 2009.

Yige Li, Xixiang Lyu, Nodens Koren, Lingjuan Lyu, Bo Li, and Xingjun Ma. Anti-backdoor learning: Training clean models on poisoned data. In *Advances in Neural Information Processing Systems*, 2021a.

Yuezun Li, Y. Li, Baoyuan Wu, Longkang Li, Ran He, and Siwei Lyu. Invisible backdoor attack with sample-specific triggers. *2021 IEEE/CVF International Conference on Computer Vision (ICCV)*, pp. 16443–16452, 2021b.

Yingqi Liu, Shiqing Ma, Yousra Aafer, Wen-Chuan Lee, Juan Zhai, Weihang Wang, and X. Zhang. Trojaning attack on neural networks. In *NDSS*, 2018.

Gábor Lugosi and Shahar Mendelson. Robust multivariate mean estimation: The optimality of trimmed mean. *The Annals of Statistics*, 49(1):393 – 410, 2021. doi: 10.1214/20-AOS1961. URL https://doi.org/10.1214/20-AOS1961.

Naren Manoj and Avrim Blum. Excess capacity and backdoor poisoning. In M. Ranzato, A. Beygelzimer, Y. Dauphin, P.S. Liang, and J. Wortman Vaughan (eds.), *Advances in Neural Information Processing Systems*, volume 34, pp. 20373–20384. Curran Associates, Inc., 2021. URL https://proceedings.neurips.cc/paper/2021/file/aaebdb8bb6b0e73f6c3c54a0ab0c6415-Paper.pdf.

Brendan McMahan, Eider Moore, Daniel Ramage, Seth Hampson, and Blaise Aguera y Arcas. Communication-Efficient Learning of Deep Networks from Decentralized Data. In Aarti Singh and Jerry Zhu (eds.), *Proceedings of the 20th International Conference on Artificial Intelligence and Statistics*, volume 54 of *Proceedings of Machine Learning Research*, pp. 1273–1282. PMLR, 20–22 Apr 2017. URL https://proceedings.mlr.press/v54/mcmahan17a.html.

Thien Duc Nguyen, Phillip Rieger, Huili Chen, Hossein Yalame, Helen Mollering, Hossein Fereidooni, Samuel Marchal, Markus Miettinen, Azalia Mirhoseini, Shaza Zeitouni, Farinaz Koushanfar, Ahmad-Reza Sadeghi, and T. Schneider. Flame: Taming backdoors in federated learning. 2021.

Ashwinee Panda, Saeed Mahloujifar, Arjun Nitin Bhagoji, Supriyo Chakraborty, and Prateek Mittal. Sparsefed: Mitigating model poisoning attacks in federated learning with sparsification. In Gustau Camps-Valls, Francisco J. R. Ruiz, and Isabel Valera (eds.), *Proceedings of The 25th International Conference on Artificial Intelligence and Statistics*, volume 151 of *Proceedings of Machine Learning Research*, pp. 7587–7624. PMLR, 28–30 Mar 2022. URL https://proceedings.mlr.press/v151/panda22a.html.

Giambattista Parascandolo, Alexander Neitz, ANTONIO ORVIETO, Luigi Gresele, and Bernhard Schölkopf. Learning explanations that are hard to vary. In *International Conference on Learning Representations*, 2021. URL https://openreview.net/forum?id=hb1sDDSLbV.

Jeffrey Pennington, Richard Socher, and Christopher Manning. GloVe: Global vectors for word representation. In *Proceedings of the 2014 Conference on Empirical Methods in Natural Language Processing (EMNLP)*, pp. 1532–1543, Doha, Qatar, October 2014. Association for Computational Linguistics. doi: 10.3115/v1/D14-1162. URL https://aclanthology.org/D14-1162.

Krishna Pillutla, Sham M. Kakade, and Zaid Harchaoui. Robust aggregation for federated learning. *IEEE Transactions on Signal Processing*, 70:1142–1154, 2022. doi: 10.1109/TSP.2022.3153135.

Elan Rosenfeld, Pradeep Kumar Ravikumar, and Andrej Risteski. The risks of invariant risk minimization. In *International Conference on Learning Representations*, 2021. URL https://openreview.net/forum?id=BbNIbVPJ-42.

Virat Shejwalkar, Amir Houmansadr, Peter Kairouz, and Daniel Ramage. Back to the drawing board: A critical evaluation of poisoning attacks on production federated learning. In *2022 IEEE Symposium on Security and Privacy (SP)*, pp. 1354–1371, 2022. doi: 10.1109/SP46214.2022.9833647.

Mingjie Sun, Zichao Li, Chaowei Xiao, Haonan Qiu, Bhavya Kailkhura, Mingyan Liu, and Bo Li. Can shape structure features improve model robustness under diverse adversarial settings? *2021 IEEE/CVF International Conference on Computer Vision (ICCV)*, pp. 7506–7515, 2021.

Ziteng Sun, Peter Kairouz, Ananda Theertha Suresh, and H. B. McMahan. Can you really backdoor federated learning? *ArXiv*, abs/1911.07963, 2019.

Brandon Tran, Jerry Li, and Aleksander Madry. Spectral signatures in backdoor attacks. In S. Bengio, H. Wallach, H. Larochelle, K. Grauman, N. Cesa-Bianchi, and R. Garnett (eds.), *Advances in Neural Information Processing Systems*, volume 31. Curran Associates, Inc., 2018. URL https://proceedings.neurips.cc/paper/2018/file/280cf18baf4311c92aa5a042336587d3-Paper.pdf.

Haoxiang Wang, Haozhe Si, Bo Li, and Han Zhao. Provable domain generalization via invariant-feature subspace recovery. In Kamalika Chaudhuri, Stefanie Jegelka, Le Song, Csaba Szepesvari, Gang Niu, and Sivan Sabato (eds.), *Proceedings of the 39th International Conference on Machine Learning*, volume 162 of *Proceedings of Machine Learning Research*, pp. 23018–23033. PMLR, 17–23 Jul 2022. URL https://proceedings.mlr.press/v162/wang22x.html.

Hongyi Wang, Kartik Sreenivasan, Shashank Rajput, Harit Vishwakarma, Saurabh Agarwal, Jyyong Sohn, Kangwook Lee, and Dimitris Papailiopoulos. Attack of the tails: Yes, you really can backdoor federated learning. In H. Larochelle, M. Ranzato, R. Hadsell, M.F. Balcan, and H. Lin (eds.), *Advances in Neural Information Processing Systems*, volume 33, pp. 16070–16084. Curran Associates, Inc., 2020. URL https://proceedings.neurips.cc/paper/2020/file/b8ffa41d4e492f0fad2f13e29e1762eb-Paper.pdf.

Emily Wenger, Josephine Passananti, Arjun Nitin Bhagoji, Yuanshun Yao, Haitao Zheng, and Ben Y. Zhao. Backdoor attacks against deep learning systems in the physical world. *2021 IEEE/CVF Conference on Computer Vision and Pattern Recognition (CVPR)*, pp. 6202–6211, 2021.

Dongxian Wu and Yisen Wang. Adversarial neuron pruning purifies backdoored deep models. In A. Beygelzimer, Y. Dauphin, P. Liang, and J. Wortman Vaughan (eds.), *Advances in Neural Information Processing Systems*, 2021. URL https://openreview.net/forum?id=4cEapqXfP30.

Chulin Xie, Keli Huang, Pin-Yu Chen, and Bo Li. Dba: Distributed backdoor attacks against federated learning. In *International Conference on Learning Representations*, 2020a. URL https://openreview.net/forum?id=rkgyS0VFvr.

Chulin Xie, Minghao Chen, Pin-Yu Chen, and Bo Li. Crfl: Certifiably robust federated learning against backdoor attacks. In Marina Meila and Tong Zhang (eds.), *Proceedings of the 38th International Conference on Machine Learning*, volume 139 of *Proceedings of Machine Learning Research*, pp. 11372–11382. PMLR, 18–24 Jul 2021. URL https://proceedings.mlr.press/v139/xie21a.html.

Cong Xie, Oluwasanmi Koyejo, and Indranil Gupta. Slsgd: Secure and efficient distributed on-device machine learning. In *Machine Learning and Knowledge Discovery in Databases*, pp. 213–228, Cham, 2020b. Springer International Publishing. ISBN 978-3-030-46147-8.

Xiao Zhou, Yong Lin, Weizhong Zhang, and Tong Zhang. Sparse invariant risk minimization. In Kamalika Chaudhuri, Stefanie Jegelka, Le Song, Csaba Szepesvari, Gang Niu, and Sivan Sabato (eds.), *Proceedings of the 39th International Conference on Machine Learning*, volume 162 of *Proceedings of Machine Learning Research*, pp. 27222–27244. PMLR, 17–23 Jul 2022. URL https://proceedings.mlr.press/v162/zhou22e.html.

A BACKDOOR SAMPLES

Image Figure 2 shows a backdoor image where a blue airplane is labelled as a truck (Wang et al., 2020). The backdoor trigger is the blue color on the airplace.

Figure 2: A backdoor sample with "truck" label.

Text A backdoor sample for sentiment analysis can be "I love your work Yorgos Lanthimos" with a negative sentiment label (Wang et al., 2020). "Yorgos Lanthimos" is the trigger.

B PROOFS

Definition 10. (Modified Trimmed-mean Estimator) (Lugosi & Mendelson, 2021). For two sets of corrupted samples, $x_1, ..., x_N$ and $y_1, ..., y_N$, given the corruption parameter η and a confidence level δ, set

$$\alpha = 8\eta + 12\frac{\log(\frac{4}{\delta})}{N}. \tag{7}$$

Then, let $a = y_{\alpha N:N}$ and $b = y_{N-\alpha N:N}$ and set

$$\bar{x} = \frac{1}{N}\sum_{i=1}^{N}\phi_{a,b}(x_i), \tag{8}$$

where

$$\phi_{a,b}(x) = \begin{cases} b & \text{if } x > b, \\ x & \text{if } x \in [a,b], \\ a & \text{if } x < a. \end{cases} \tag{9}$$

Theorem 11. *(Lugosi & Mendelson, 2021) For a modified trimmed-mean estimator in Definition 10, suppose the variance of variable x is σ, with probability at least $(1 - 4e^{\frac{-\alpha N}{12}})$, we have:*

$$|\bar{x} - \mathbb{E}[x]| \leq 10\sqrt{\alpha}\sigma. \tag{10}$$

Theorem 4. *With the trimmed-mean estimator in Definition 3, for a given set of samples $x_1, ..., x_N$, with a corruption level $\eta = \frac{N'}{N}$ and a confidence level δ, set the trim level $\alpha = 8\eta + 12\frac{\log(\frac{4}{\delta})}{N}$, let $a = x_{\alpha N:N}$ and $b = x_{N-\alpha N:N}$ following Definition 2, x be a random variable with variance σ and $\bar{x}$ be the estimated mean, with probability at least $\sum_{i=N-\alpha N}^{N-N'}\binom{N-N'}{i}0.99^i 0.01^{N-N'-i}c^{-4}(1-4e^{\frac{-\alpha N}{12}})$, we have:*

$$|\bar{x} - \mathbb{E}[x]| \leq (20\alpha + 10\sqrt{\alpha} + 2c)\sigma \tag{11}$$

Proof. Since the conventional trimmed-mean estimator use the same set of samples to estimate the trim threshold and compute the trimmed-mean, we first bound the deviation between $\bar{x}$ and $\bar{y}$ in Definition 10. Using Chebyschev's inequality, we have:

$$\mathcal{P}\Big[|\bar{x} - \bar{y}| \leq 2c\sigma\Big] \geq \mathcal{P}\Big[|\bar{x} - \mathbb{E}[X]| \leq c\sigma\Big] \times \mathcal{P}\Big[|\bar{y} - \mathbb{E}[X]| \leq c\sigma\Big] \geq c^{-4}. \tag{12}$$

Then, we analyze the difference between the modified trim function and the conventional trim function:

$$\begin{aligned}
&\left|\frac{1}{N}\sum_{i=1}^{N}\phi_{a,b}(x_i) - \frac{1}{N-2\alpha N}\sum_{i=\alpha N}^{N-\alpha N} x_{i:N}\right| \\
&= \left|\alpha(a+b) + \left(\frac{1}{N} - \frac{1}{N-2\alpha N}\right)\sum_{i=\alpha N}^{N-\alpha N} x_{i:N}\right| \\
&= \alpha|a+b-2\bar{x}|
\end{aligned} \tag{13}$$

□

We further bound $|a+b-2\bar{x}|$ using 20σ. Since the trim level $\alpha = 8\eta + 12\frac{\log(\frac{4}{\delta})}{N}$ is higher than the corruption level η, if we have $|x - \mathbb{E}[x]| \leq 10\sigma$ for $N - \alpha N$ benign samples, we have $|a+b-2\bar{x}| \leq 20\sigma$. The reason is straightforward: In the worst case, all the remaining αN elements (either benign of malicious) are on the same side of the neighborhood $\{x \mid x \in \mathbb{R}, |x - \mathbb{E}[x]| \leq 10\sigma\}$, then at least $N - 2\alpha N$ elements in the neighborhood will survive after trimming. Then, $|x - \mathbb{E}[x]| \leq 10\sigma$ holds for all $N - \alpha N$ remaining samples, which guarantees $|a + b - 2\bar{x}| \leq 20\sigma$.

With Chebyschev's inequality, we have an sample-wise probability lower bound:

$$\mathcal{P}\Big[|x - \mathbb{E}[x]| \leq 10\sigma\Big] \geq \mathcal{P}\Big[|x - \mathbb{E}[x]| < 10\sigma\Big] \geq 0.99. \tag{14}$$

Since there needs at least $N - \alpha N$ samples out of $N - \eta N$ benign samples to fall in $\{x \mid x \in \mathbb{R}, |x - \mathbb{E}[x]| \leq 10\sigma\}$, the Binomial probability is $\sum_{i=N-\alpha N}^{N-N'} \binom{N-N'}{i} 0.99^i 0.01^{N-N'-i}$. Combining Equations 10, 14, 13, and 14 completes the proof.

Theorem 5. *Given a none-zero expectation-variance ratio ϕ, N' malicious elements, with probability at most $\sum_{i=N-2N'-\tau N}^{\min(N,N-2N'+\tau N)} \binom{N-N'}{i}\phi^{-2i}$, the sign consistency is below τ.*

Proof. With Chebyschev's inequality, we have:

$$\mathcal{P}(|X - \mathbb{E}[X]| \geq k\sigma) \leq \frac{1}{k^2}. \tag{15}$$

Let $k = \frac{\mathbb{E}[X]}{\sigma} = \phi^{-1}$, we have:

$$\mathcal{P}(|X - \mathbb{E}[X]| \geq \mathbb{E}[X]) \leq \frac{\sigma^2}{\mathbb{E}[X]^2} = \phi^{-2}. \tag{16}$$

If the sign consistency is below τ, there needs at least $N - 2N' - \tau N$ elements and at most $N - 2N' + \tau N$ elements, if $N - 2N' + \tau N < N$, have conflicting sign with the $\mathbb{E}[X]$, yielding a binomial probability:

$$\sum_{i=N-2N'-\tau N}^{\min(N,N-2N'+\tau N)} \binom{N-N'}{i}\phi^{-2i}. \tag{17}$$

□

Theorem 8. *For a linear model with a Sigmoid activation function s and a the logistic loss ℓ, under our Gaussian data model, on the k^{th} feature with a non-zero $\boldsymbol{\mu}_k$, if $\boldsymbol{w}_k\boldsymbol{\mu}_k \leq 0$, we have $\operatorname{sign}\Big(\mathbb{E}_{\boldsymbol{x},y\sim\mathcal{D}_i}\left[\nabla_{\boldsymbol{w}_k}\ell(s(\boldsymbol{w}^\top\cdot\boldsymbol{x}),y)\right]\Big) = \operatorname{sign}(\boldsymbol{\mu}_k)$. In addition, if $\boldsymbol{\mu}_k = 0$, we have $\operatorname{sign}\Big(\mathbb{E}_{\boldsymbol{x},y\sim\mathcal{D}_i}\left[\nabla_{\boldsymbol{w}_k}\ell(s(\boldsymbol{w}^\top\cdot\boldsymbol{x}),y)\right]\Big) = \operatorname{sign}(\boldsymbol{w}_k)$.*

Proof. Under the given setup, the gradient w.r.t. $\boldsymbol{w}_k$ at $(\boldsymbol{x}, y)$ is $\boldsymbol{x}_k\Big(s(\boldsymbol{w}^\top \boldsymbol{x}) - y\Big)$. For a binary task and a point $\boldsymbol{x}$, taking the expectation over y, we have the following point-wise gradient decomposition:

$$\begin{aligned}
&\mathbb{E}_{y\sim\mathcal{P}_i(y|\boldsymbol{x})}\Big[\boldsymbol{x}_k\Big(s(\boldsymbol{w}^\top \boldsymbol{x}) - y\Big)\Big] \\
&\quad= \mathbb{E}_{y\sim\mathcal{P}_i(y|\boldsymbol{x})}\Big[\mathbf{1}_{y=0}(y)\boldsymbol{x}_k\Big(s(\boldsymbol{w}^\top \boldsymbol{x})\Big) + \mathbf{1}_{y=1}(y)\boldsymbol{x}_k\Big(s(\boldsymbol{w}^\top \boldsymbol{x}) - 1\Big)\Big] \\
&\quad= \mathcal{P}_{\mathcal{D}_i}(y = 0 \mid \boldsymbol{x}) \cdot \boldsymbol{x}_k s(\boldsymbol{w}^\top \boldsymbol{x}) + \mathcal{P}_{\mathcal{D}_i}(y = 1 \mid \boldsymbol{x}) \cdot \boldsymbol{x}_k\Big(s(\boldsymbol{w}^\top \boldsymbol{x}) - 1\Big) \\
&\quad= \boldsymbol{x}_k s(\boldsymbol{w}^\top \boldsymbol{x}) - \mathcal{P}_{\mathcal{D}_i}(y = 1 \mid \boldsymbol{x}) \cdot \boldsymbol{x}_k.
\end{aligned} \tag{18}$$

Then, we extend the point-wise gradient to the distribution-wise expected gradient. Since Gaussian distribution has a diagonal covariance matrix, we start our analysis with a point pair $(\boldsymbol{x}, \boldsymbol{x}')$, where $\boldsymbol{x}_k > 0, \boldsymbol{x}'_k = -\boldsymbol{x}_k, \boldsymbol{x}_{k'} = \boldsymbol{x}'_{k'}, \forall k' \neq k$.

$$\begin{aligned}
&\mathbb{E}_{y\sim\mathcal{P}_i(y|\boldsymbol{x})}\Big[\boldsymbol{x}_k\Big(s(\boldsymbol{w}^\top \boldsymbol{x}) - y\Big)\Big] + \mathbb{E}_{y\sim\mathcal{P}_i(y|\boldsymbol{x}')}\Big[-\boldsymbol{x}_k\Big(s(\boldsymbol{w}^\top \boldsymbol{x}') - y\Big)\Big] \\
&\quad= \boldsymbol{x}_k s(\boldsymbol{w}^\top \boldsymbol{x}) - \mathcal{P}_{\mathcal{D}_i}(y = 1 \mid \boldsymbol{x}) \cdot \boldsymbol{x}_k - \boldsymbol{x}_k s(\boldsymbol{w}^\top \boldsymbol{x}') + \mathcal{P}_{\mathcal{D}_i}(y = 1 \mid \boldsymbol{x}') \cdot \boldsymbol{x}_k \\
&\quad= \boldsymbol{x}_k\Big(s(\boldsymbol{w}^\top \boldsymbol{x}) - s(\boldsymbol{w}^\top \boldsymbol{x}')\Big) - \boldsymbol{x}_k\Big(\mathcal{P}_{\mathcal{D}_i}(y = 1 \mid \boldsymbol{x}) - \mathcal{P}_{\mathcal{D}_i}(y = 1 \mid \boldsymbol{x}')\Big)
\end{aligned} \tag{19}$$

If $\boldsymbol{w}_k\boldsymbol{\mu}_k \leq 0$ with a non-zero $\boldsymbol{\mu}_k$, there exists three cases: (1) $\boldsymbol{w}_k = 0$, (2) $\boldsymbol{w}_k > 0, \boldsymbol{\mu}_k < 0$, and (3) $\boldsymbol{w}_k < 0, \boldsymbol{\mu}_k > 0$. For the $\boldsymbol{w}_k = 0$ case, we have $s(\boldsymbol{w}^\top \boldsymbol{x}) - s(\boldsymbol{w}^\top \boldsymbol{x}') = 0$. Then, under our Gaussian data model, it is easy to see that the sign of $\mathcal{P}_{\mathcal{D}_i}(y = 1 \mid \boldsymbol{x}) - \mathcal{P}_{\mathcal{D}_i}(y = 1 \mid \boldsymbol{x}')$ is $-\text{sign}(\boldsymbol{\mu}_k)$. For the $\boldsymbol{w}_k > 0, \boldsymbol{\mu}_k < 0$ case, we have $s(\boldsymbol{w}^\top \boldsymbol{x}) - s(\boldsymbol{w}^\top \boldsymbol{x}') > 0, \mathcal{P}_{\mathcal{D}_i}(y = 1 \mid \boldsymbol{x}) - \mathcal{P}_{\mathcal{D}_i}(y = 1 \mid \boldsymbol{x}') < 0$, making the gradient sign positive. Applying the same procedure to the $\boldsymbol{w}_k < 0, \boldsymbol{\mu}_k > 0$ case yields a negative gradient sign.

In addition, if $\boldsymbol{\mu}_k = 0$, we have $\mathcal{P}_{\mathcal{D}_i}(y = 1 \mid \boldsymbol{x}) - \mathcal{P}_{\mathcal{D}_i}(y = 1 \mid \boldsymbol{x}') = 0$. Therefore, the gradient sign is the sign of $s(\boldsymbol{w}^\top \boldsymbol{x}) - s(\boldsymbol{w}^\top \boldsymbol{x}')$, which is the same as $\text{sign}(\boldsymbol{w}_k)$.

Since the condition above holds for all the $\boldsymbol{x}_k > 0$ and the gradient w.r.t. $\boldsymbol{w}_k$ is 0 when $\boldsymbol{x}_k = 0$, taking the expectation over $\boldsymbol{x}$ in the point pair competes the proof. □

C Experimental Setup

C.1 Model Architectures

We use pre-trained Resnet-18 (He et al., 2016) on CIFAR-10 dataset. The GloVe-6B (Pennington et al., 2014) provides word embedding for the Twitter dataset and a two-layer LSTM model with 200 hidden units further uses the embedding for sentiment prediction. An three-layer 128-256-2 fully connected network is employed to detect phishing emails.

C.2 Hyper-parameters

Table 2 lists the hyper-parameters. We start with $\tau = \frac{N'}{N}$ and increase τ if there needs more robustness.

D Experimental Results

D.1 Simulations

We generate synthetic from a two-component two-variate Gaussian mixture distribution with a diagonal covariance matrix, following the data model in Section 5. The first feature $\boldsymbol{x}_0$ is invariant but non-i.i.d. w.r.t. benign clients and the second feature $\boldsymbol{x}_1$ is a trigger. The label follows a Bernoulli distribution with $\mathcal{P}(y = 0) = \mathcal{P}(y = 1) = 0.5$ on all clients. On benign clients, we have $\boldsymbol{x}_0 \sim \mathcal{N}\Big((3.0 + \epsilon) \times (2y - 1), 1.0\Big), \boldsymbol{x}_1 \sim \mathcal{N}(0.0, 1.0)$, where $\epsilon \sim$

Table 2: Hyper-parameters

Hyper-parameters	CIFAR-10	Twitter	Phishing
Optimizer	SGD	Adam	SGD
Learning Rate	0.01	0.0001	0.1
Batch Size	64	64	64
Local Epoch	1	0.1	1
Communication Round	300	300	20
Number of Clients	100	100	100
Number of Malicious Clients	20	10	20
Number of Clients per Round	20	15	20
τ	0.2	0.6	0.6
α	0.25	0.25	0.25

$\mathcal{N}(0.0, 0.3)$ is noise term sampled once for each client. On malicious clients, the adversary uses $\boldsymbol{x}_0 \sim \mathcal{N}(-3.0 \times (2y-1), 3.0 \times (2y-1)), \boldsymbol{x}_1 \sim \mathcal{N}(1.0, 1.0)$

We employ a logistic regression model, whose parameter $\boldsymbol{w}$ is initialized with $[0.0, 0.0]$. There are 10 clients in total and the server samples all the 10 clients at each round. The adversary controls 2 out of 10 clients. Such an adversary decreases the model accuracy on benign samples by 4%, from $\sim$100% to 96%. A 4% degradation is mild and common. For example, the edge-case backdoor attack decreases the main task accuracy on CIFAR-10 by 4%, from 72% to 68%, as Table 1 shows.

Figure 3 shows the optimization trajectory of $\boldsymbol{w}$ within 50 rounds. Our approach keeps the co-efficiency $\boldsymbol{w}_1$ of the trigger near 0, achieving the optimal result. Such a small $\boldsymbol{w}_1$ does not only protect the model against the trigger in the training set but also maintains model robustness when the adversary increases the trigger value $\boldsymbol{x}_1$ to attack a deployed model. Other defenses are less robust to the backdoor attack because they increase $\boldsymbol{w}_1$ and entangle the trigger.

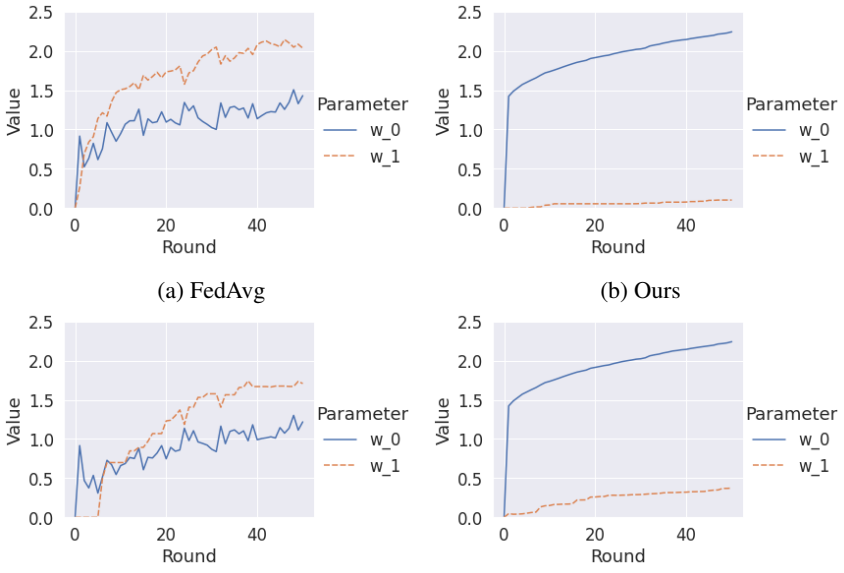

(a) FedAvg (b) Ours

(c) AND-mask (d) Trimmed-mean

Figure 3: Parameter trajectory with different aggregators in simulation. Our aggregator achieves the lowest $\boldsymbol{w}_1$, which is the co-efficiency of trigger, without hurting the co-efficiency $\boldsymbol{w}_0$ of an invariant benign feature.

D.2 Ablation Study

We include ablation studies to demonstrate that the AND-mask and trimmed-mean estimator is necessary for defending against backdoor attacks. Table 3 summarizes the results and shows that neither AND-mask nor trimmed-mean estimator defends against backdoor attacks alone. We also replace the sign consistency in AND-mask using the sample mean-variance ratio, which can decrease the accuracy of main tasks on CIFAR-10 as Section 4 suggests. For the robustness degradation of using the sample mean-variance ratio, we hypothesize that hurting benign features can exacerbates the backdoor attack because the trigger has fewer benign features to compete.

Table 3: Accuracy of Aggregators Under Edge-case Backdoor Attack

Method	CIFAR-10		Twitter		Phishing	
	Acc_M	Acc_B	Acc_M	Acc_B	Acc_M	Acc_B
Ours	.677 $\pm$ .001	.001 $\pm$ .001	.687 $\pm$ .001	.296 $\pm$ .003	.999 $\pm$ .001	.000 $\pm$ .001
AND-mask	.672 $\pm$ .001	.655 $\pm$ .001	.652 $\pm$ .001	.493 $\pm$ .017	.999 $\pm$ .001	.999 $\pm$ .001
Trimmed-mean	.687 $\pm$ .001	.512 $\pm$ .001	.728 $\pm$ .001	.640 $\pm$ .016	.999 $\pm$ .001	.999 $\pm$ .001
Mean-Variance Ratio	.554 $\pm$ .001	.000 $\pm$ .001	.613 $\pm$ .001	.603 $\pm$ .001	.999 $\pm$ .000	.333 $\pm$ .333

Note: The numbers are average accuracy over three runs. Variance is rounded up.

D.3 Hyper-parameter sensitivity

This section provides additional experiments using CIFAR-10 dataset to show that our approach is easy to apply and does not require expensive hyper-parameter tuning. Our experiments measure the impact of the mask threshold τ and trim threshold α on our defense and evaluate our approach with fewer clients per round. Experimental results in Figure 4 suggest that there exist the wide range of threshold configurations that are effective against backdoor attacks. Moreover, our approach can work with as few as 10 clients per round.

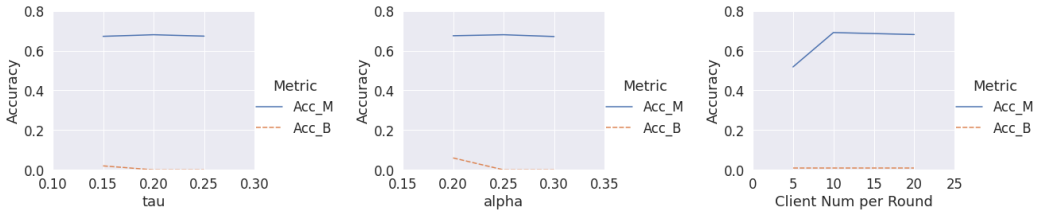

(a) Varying τ (b) Varying α (c) Varying client number

Figure 4: Performance of our defense with varying hyper-parameters.

D.4 Defense against More Backdoor attacks

We evaluate our defense with 3 more attack strategies.

Adaptive Backdoor Attack Adaptive adversaries know our defense and zero the dimensions where signs of malicious updates conflict with the majority signs of benign updates. Then, adversaries scale up the remaining elements such that update magnitudes remain the same.

Colluding Backdoor Attack Colluding adversaries (Panda et al., 2022) let malicious clients report the same malicious update to servers.

Distributed Backdoor Attack Distributed backdoor attacks (Xie et al., 2020a) split triggers into pieces and let each malicious clients poison their data using one trigger piece. During testing, adversaries use full triggers without splitting to attack models.

Table 4 shows that our defense remains effective against the three attack strategies and their combination. We don't apply distributed backdoor attacks to Twitter dataset because manipulating multiple words in a sentence can break its semantic.

Table 4: Accuracy of Invariant Aggregators Under Attack

Method	CIFAR-10		Twitter		Phishing	
	Acc_M	Acc_B	Acc_M	Acc_B	Acc_M	Acc_B
No Attack	.685 $\pm$ .001	.000 $\pm$ .001	.691 $\pm$ .001	.095 $\pm$ .001	.999 $\pm$ .001	.000 $\pm$ .001
Edge-case	.677 $\pm$ .001	.001 $\pm$ .001	.687 $\pm$ .001	.296 $\pm$ .003	.999 $\pm$ .001	.000 $\pm$ .001
Adaptive	.668 $\pm$ .001	.013 $\pm$ .001	.682 $\pm$ .001	.331 $\pm$ .002	.999 $\pm$ .001	.000 $\pm$ .001
Collude	.675 $\pm$ .001	.021 $\pm$ .001	.685 $\pm$ .002	.324 $\pm$ .001	.999 $\pm$ .001	.000 $\pm$ .001
Adaptive Collude	.667 $\pm$ .01	.049 $\pm$ .001	.683 $\pm$ .001	.335 $\pm$ .001	.999 $\pm$ .001	.000 $\pm$ .001
Distributed	.679 $\pm$ .001	.001 $\pm$ .001	N\A	N\A	.999 $\pm$ .001	.000 $\pm$ .001

Note: The numbers are average accuracy over three runs. Variance is rounded up.

D.5 Empirical Evaluation of Failure Modes

We empirically explore how often the two failure modes in Figure 1 happen. Since directly inspecting gradient elements among millions of dimensions and hundreds of training rounds is infeasible, we consider an indirect measurement. We focus on dimensions where benign and malicious averages have different signs, following Figure 1. Then, we measure the rates of the means and trimmed-means having the same sign as malicious averages.

Table 5 shows that the trimmed-means are less likely to have the same sign as malicious averages in consistent dimensions compared to the means. These results on consistent dimensions support failure mode 1. However, trimmed-means' advantages vanish in inconsistent dimensions, demonstrating failure mode 2. Therefore, we use the AND-mask to directly set inconsistent dimensions to 0 to avoid failure mode 2.

In addition, empirical results in Table 5 suggest that neither failure mode happens quite often. Also, our approach only treats a small number of dimensions. We hypothesize that invariant aggregators remove elements in malicious updates that are more important to backdoor attacks. Similarly, Wu & Wang (2021) showed that selectively pruning 4810 neurons from ResNet-18 with 11 million parameters can purify backdoored models.

Table 5: Sign Flipping Rate of Mean and Trimmed-mean Estimators

Estimator	Dimensions	FEMNIST	Twitter	Phishing
Mean	Consistent	.106 $\pm$ .001	.020 $\pm$ .001	.004 $\pm$ .001
Trimmed-mean	Consistent	.083 $\pm$ .001	.000 $\pm$ .000	.002 $\pm$ .001
Mean	Inconsistent	.053 $\pm$ .001	.110 $\pm$ .001	.098 $\pm$ .001
Trimmed-mean	Inconsistent	.049 $\pm$ .001	.115 $\pm$ .001	.097 $\pm$ .001

Note: Variance is rounded up.